Journal of Porous Materials (2019) 26:381–387
https://doi.org/10.1007/s10934-018-0612-5

Metal organic framework-derived Ni/Zn/Co/NC composites as efficient catalyst for oxygen evolution reaction

Shengyun Zhao[1,3] · **Juan Chen**[2]

Published online: 20 April 2018

Abstract
Electrocatalytic water splitting to acquire hydrogen has been recognized as one of the most promising routes to solve the energy crisis and environmental issues. In this paper, we adopted the facile cocrystallization technique to synthesize the ZIF-8/ZIF-67 and used it as support to prepare Ni/ZIF-8/ZIF-67. After being annealed at 800 °C, Ni/ZIF-8/ZIF-67 was successfully transformed into Ni/Zn/Co/NC electrocatalyst (NC is the abbreviation of nitrogen-doped graphitic carbon). The structures and properties of all as-synthesized samples were characterized by X-ray diffraction (XRD), scanning electron microscopy (SEM), energy dispersive spectroscopy (EDS), transmission electron microscope (TEM). The oxygen evolution reaction (OER) activity was evaluated in a standard three-electrode electrochemical cell in alkaline solution (1 M KOH solution). The results show that the doping of Ni and Zn has great influence on the OER activity of Co/NC electrocatalyst. Compared with Co/NC (1.63 V) and Zn/Co/NC (1.58 V), Ni/Zn/Co/NC exhibits the highest OER activity (1.53 V). Except that, Ni/Zn/Co/NC has high stability. After 10 h of continuous operation at a static potential of 1.52 V for 10 h, it just shows 4.0% of decay.

Keywords ZIF-8 · ZIF-67 · Ni · Zn · Co · NC · Oxygen evolution reaction

1 Introduction

With the development of modern society, fossil energy has been widely used. The excessive consumption of the fossil energy causes the serious environmental issues, such as acid rain, global warming and ozone depletion [1–3]. Furthermore, the fossil energy is limited. The energy crisis and environment issues makes it urgent to develop clean and sustainable energy sources. Until now, there are many clean and sustainable energy sources, such as wind, water and solar power [4–6]. Among them. solar energy is a kind of sustainable fuel, which can provide a nearly endless supply and can be utilized to split water, producing H_2 and O_2 [7, 8]. Splitting water to obtain H_2 not only can solve the global warming issue but also decrease the demand for fossil energy. Recent years, many effects have been made to develop catalysts with efficient performances [9, 10]. Among these catalysts, IrO_2 and RuO_2 show excellent OER properties [11, 12]. But IrO_2 and RuO_2 are easy to be oxidized and their high costs limit their practical applications [13]. Thus, it is urgent to develop a kind of inexpensive catalysts which are easy to be applied and have excellent properties.

Zeolitic imidazolate frameworks (ZIFs), as a kind of MOFs, is constructed by metal ion(II) and 2-methylimidazole ligands. The most widely ZIFs is ZIF-67, which is constructed by Co(II) and 2-methylimidazole ligands [14]. Due to the high specific surface area, uniform channels, and regular pores, it is widely used in various catalytic fields, such as the hydrogenation of alkenes [15], knoevenagel condensation reaction [16] and the semihydrogenation of phenylacetylene [17]. Furthermore, ZIF-67 has been demonstrated to be a promising precursor to prepare electrocatalysts with high performance. Liu et al. used carbon cloth (CC) as support to load a lay of ZIF-67 and employed it to prepare Co–P/NC/CC by annealing it at 900 °C for 3 h under flowing argon [18]. They found that Co–P/NC/CC catalyst

✉ Juan Chen
chenjuan_xm@hotmail.com

1 College of Ecology and Resource Engineering, Wuyi University, Wuyishan 354300, Fujian, China

2 Department of Pharmacy, Zhongshan Hospital, Xiamen University, Xiamen 361004, China

3 Fujian Provincial Key Laboratory of Eco-Inductrial Green Technology, Wuyi University, Wuyishan 354300, Fujian, China

exhibited remarkable catalytic performance in 1 M KOH with Tafel slopes of 52 and 61 mV/dec for HER and OER, respectively. Li et al. adopted ZIF-67 as precursor to prepare Co–NC@CoP–NC nanopolyhedra and found that Co–NC@CoP–NC nanopolyhedra has excellent activity and satbility for both the OER and ORR [19]. Guan et al. used PS@ZIF-67 as precursor to obtain Co/NC hollow particles by a controlled pyrolysis [20]. The synthesized Co/NC manifest superior electrocatalytic oxygen reduction performance with high activity and excellent durability.

ZIF-8, as another ZIFs, is constructed by Zn(II) and 2-methylimidazole ligands [21]. It has the same structure with ZIF-67 and can conjugate with ZIF-67 to synthesize ZIF-8/ZIF-67 hybrid catalyst. Here, ZIF-8/ZIF-67 composites were firstly synthesized through the facile cocrystallization technique. And it was used as support to load Ni element. Ni/Zn/Co/NC, Ni, Zn, Co and N co-doped graphitic carbon, was successfully fabricated through carbonization of Ni/ZIF-8/ZIF-67. Ni, Zn, Co and N elements were well dispersed on porous graphitic carbon. The as-synthesized Ni/Zn/Co/NC was used as electrocatalyst to text its oxygen evolution reaction (OER) activity in a standard three-electrode electrochemical cell in alkaline solution (1 M KOH solution). After evolution, it shows excellent electrocatalytic activity with an overpotential of 285 mV at the current density of 10 mA/cm^2 and exhibits great durability during the long-term stability test. The excellent properties of Ni/Zn/Co/NC electrocatalyst makes it potential to be used in splitting water to obtain H_2.

2 Experimental

2.1 Chemicals

Zinc nitrate hexahydrate [$Zn(NO_3)_2{\cdot}6H_2O$], cobalt nitrate hexahydrate [$Co(NO_3)_2{\cdot}6H_2O$], nickel nitrate hexahydrate [$Ni(NO_3)_2{\cdot}6H_2O$], 2-methylimidazole [2-Hmim] and methanol were all purchased from Sinopharm Chemical Reagent Co. Ltd. All the chemical reagents used in this study are of analytical grade and used directly without any further purification. Distilled water was used in this experiment.

2.2 Synthesis of Ni/Zn/Co/NC catalyst

In this experiment, Ni/Zn/Co/NC was synthesized by the following procedures. First, ZIF-8/ZIF-67 was synthesized by mixing Co^{2+} and Zn^{2+} with 2-methylimidazole, as reported in the previous literature [21]. 8 mmol $Zn(NO_3)_2{\cdot}6H_2O$ and 2 mmol $Co(NO_3)_2{\cdot}6H_2O$ was dissolved into 100 mL methanol together and kept stirring for 10 min, which was labeled as (A) 40 mmol 2-methylimidazole (2-Hmim), was dissolved 100 mL methanol, which was marked as (B) And B solution was poured into the A solution slowly and kept stirring for 10 min. Then, the mixture was left to stand for 24 h at room temperature. And the mixture was centrifuged, washed with methanol and dried at 70 °C to obtain ZIF-8/ZIF-67 nanoparticles. After that, 0.5 g ZIF-8/ZIF-67 was dispersed into 100 ml methanol solution, which contained 0.5 g $Ni(NO_3)_2{\cdot}6H_2O$. The suspension kept stirring for 30 min and dried at 80 °C to get Ni-doped ZIF-8/ZIF-67. Finally, the Ni-doped ZIF-8/ZIF-67 was annealed at 800 °C in the Ar atmosphere for 6 h to obtain the Ni/Zn/Co/NC catalyst. For comparison, Co/NC and Zn/Co/NC were prepared by annealing ZIF-67 and ZIF-8/ZIF-67 at 800 °C in the Ar atmosphere for 6 h. The formation mechanism of Ni/Zn/Co/NC is shown in Fig. 1.

2.3 Characterization

The powder X-ray diffraction (XRD) patterns of all as-synthesized samples were recorded no a Shimadzu X-ray diffractometer (Model 6000) using Cu K*a* radiation, operated at 40 kV and 40 mA. The scanning electron microscope (SEM) images were observed by field emission scanning electron microscopy (SEM) on Hitachi SU-70. The energy dispersive spectroscopy (EDS) mappings were obtained on Hitachi SU-70 at 20 kV. The transmission electron microscopy (TEM) images were recorded on a Hitachi HT-7700 transmission electron microscopy at an accelerating voltage of 200 kV.

2.4 Electrochemical measurements

The electrochemical tests of all samples were performed on a standard three-electrode cell. Pt wire and Ag/AgCl were

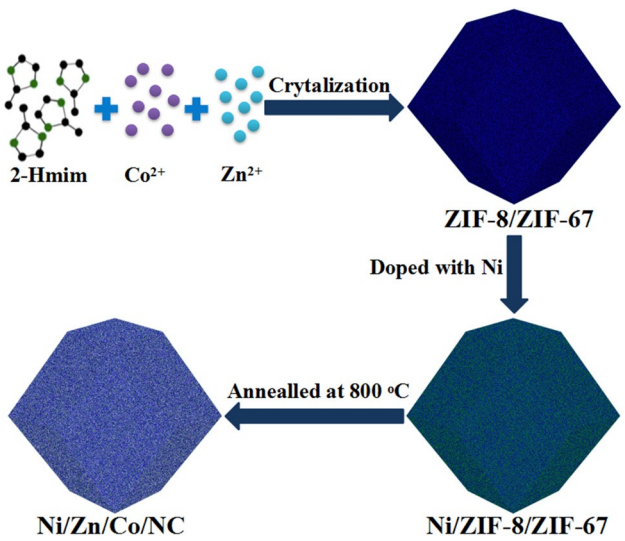

Fig. 1 Schematic illustration of the synthesis of Ni/Co/NC catalyst

used as counter and reference electrodes, respectively. 8 mg sample was dispersed in 600 µL water/ethanol (14/1 v/v) mixture containing 60 µL Nafion solution (5 wt%) to form a homogeneous suspension. Then, the as formed suspension was dropped into the glassy-carbon disk and dried for the oxygen evolution reaction measurement at room temperature. In order to stabilize the signals, the working electrode was scanned for 20–30 cycles of cyclic voltammetry (CV) before the OER measurement. The polarization curves were recorded at a slow scan rate of 10 mV/s. During the measurement, a flow of O_2 was maintained to ensure the O_2/H_2O equilibrium at 1.23 V versus RHE. In the 1 M KOH aqeous solution, E versus RHE = E versus Ag/AgCl + 0.0591 × pH + 0.197 V. The overpotential (η) for OER is η = E versus. RHE-1.23 V = E versus Ag/AgCl + 0.0591 × pH + 0.197 V.

3 Results and discussion

The synthesized ZIF-67, ZIF-8/ZIF-67 and Ni/ZIF-8/ZIF-67 was observed on Hitachi SU-70. The results are shown in Fig. 2. From Fig. 2, all samples exhibit rhombic dodecahedron morphology. The particles size of ZIF-67 is about 550 nm (Fig. 2a). When Co^{2+} and Zn^{2+} mix with 2-methylimidazole, they can coordinate with 2-methylimidazole ligands to form ZIF-8/ZIF-67 [21]. The particle size of ZIF-8/ZIF-67 is about 400 nm (Fig. 2b), which is smaller than ZIF-8. This result is in accordance with Zaręba's reports [22]. Figure 2c is the SEM image of Ni/ZIF-8/ZIF-67. The doping of Ni did not destroy the morphology of ZIF-8/ZIF-67. Figure 2d shows the XRD patterns of ZIF-67, ZIF-8/ZIF-67 and Ni/ZIF-8/ZIF-67. All samples exhibit the same peaks at 7.38°, 10.48°, 12.76°, 14.75°, 16.49° and 18.06°, which are ascribed to (011), (002), (112), (022), (013) and (222) reflections of ZIF-67 (JCPDS: 89-3739) [23]. ZIF-8/ZIF-67 has the same structure with ZIF-67. There are no appearing other new peaks in Ni/ZIF-8/ZIF-67. It reveals that the doping of Ni does not change the structure of ZIF-8/ZIF-67.

In order to remove the organic ligands, ZIF-67, ZIF-8/ZIF-67 and Ni/ZIF-8/ZIF-67 were annealed at 800 °C in the Ar atmosphere to prepare Co/NC, Zn/Co/NC and Ni/Zn/Co/NC, respectively. The XRD patterns of Co/NC, Zn/Co/NC, Ni/Co/NC are shown in Fig. 3a. All samples show a weak peak at 26.1°, which is ascribed to the diffraction of carbon. Except that, there are existing peaks at 44.3° and 51.7°, which are ascribed to (111) and (200) reflections of Co [24]. The XRD patterns of Zn/Co/NC and Ni/Zn/Co/NC are almost the same with the XRD patterns of Co/NC. It indicates that the doped of Zn and Ni did not change the structure of Co/NC. Figure 3b is the Raman spectrum of Co/NC. The Raman spectrum of Co/NC shows the peaks at 1360/cm for the D band and at 1587/cm for the G band, in which the high-intensity G peak reveals a high-graphitization degree [25].

Figure 4 shows the SEM images of Co/NC, Zn/Co/NC, Ni/Co/NC and TEM images of Ni/Co/NC. Figure 4a is the SEM image of Co/NC. Parts of the structure is broke down. The particle size of Co/NC is about 100 nm. When ZIF-67 is doped with Zn (ZIF-8/ZIF-67) and annealed

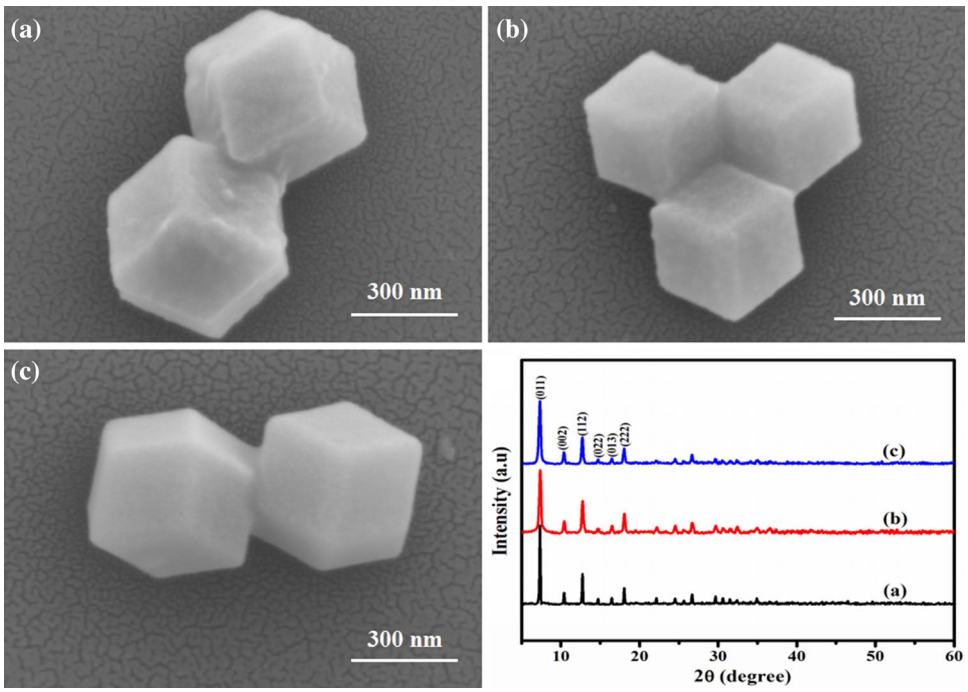

Fig. 2 SEM images of **a** ZIF-67, **b** ZIF-8/ZIF-67, **c** Ni/ZIF-8/ZIF-67 and the XRD patterns

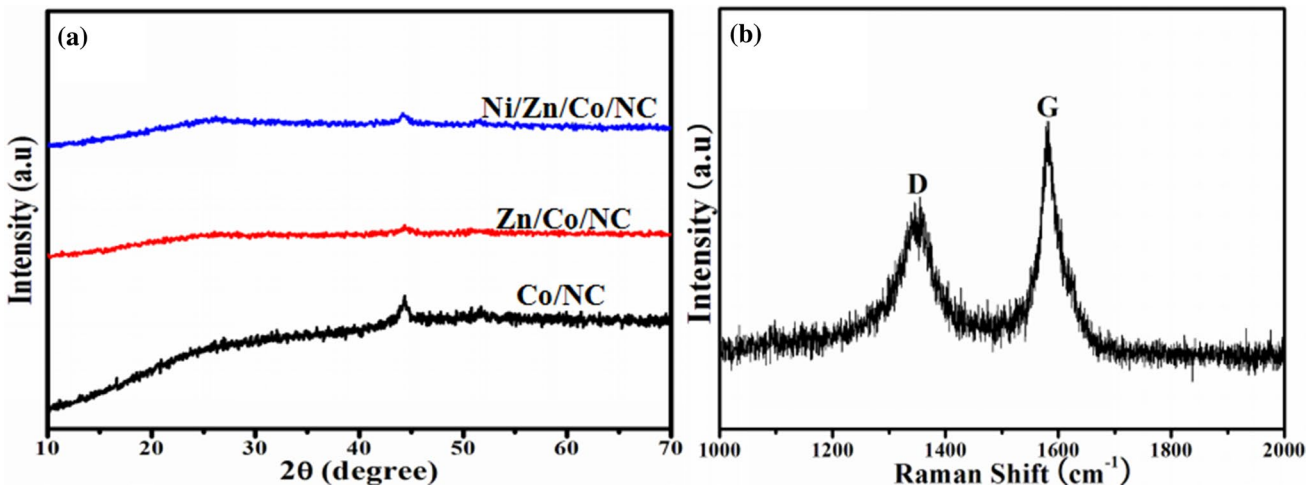

Fig. 3 **a** XRD patterns of Co/NC, Zn/Co/NC, Ni/Zn/Co/NC and **b** Raman spectrum of Co/NC

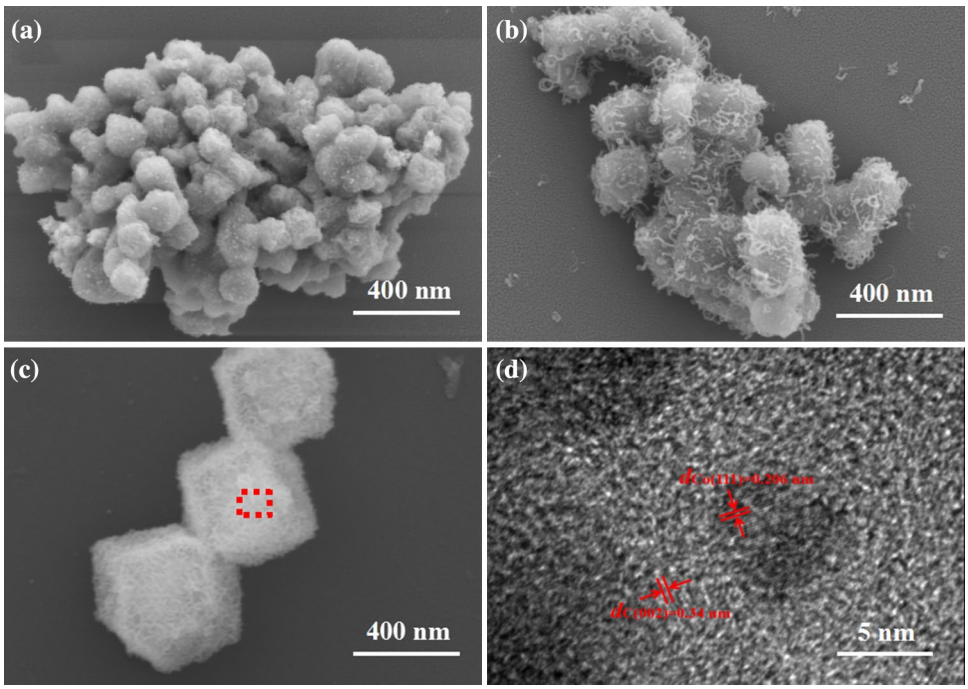

Fig. 4 SEM images of **a** Co/NC, **b** Zn/Co/NC, **c** Ni/Co/NC and **d** TEM image of Ni/Co/NC

at 800 °C in the Ar atmosphere to form Zn/Co/NC, the structure is broke down and its surface is surrounded by carbon nanowires (Fig. 3b). Figure 3c is the SEM image of Ni/Zn/Co/NC. It can be seen that Ni/Zn/Co/NC nanoparticles show more dodecahedral than Co/NC and Zn/Co/NC. From the previous research, we can know that Ni element, adhering on the surface and/or in the pore canals of ZIF-67, can act as support to protect its morphology. Figure 3d is the the high-resolution transmission electron microscopy (HRTEM) of Ni/Zn/Co/NC. Ni/Zn/Co/NC nanoparticles exist a porous structure, in which many black dots, with the lattice fringe of 0.206 nm, are embedded. The lattice fringe of 0.206 nm is corresponding to the (111) planes of Co. Except that, there is also existing the distinct lattice fringe of 0.34 nm, which is corresponded to the (002) lattice plane of carbon. The bent graphitic layers can also be directly observed, indicating the graphitization of carbon.

From the XRD patterns and the TEM image of Ni/Co/NC (Figs. 3c, 4d), we can know that Ni/Co/NC exists porous carbon and Co. In order to investigate the doping of Zn and Ni element, Ni/Zn/Co/NC were analyzed by EDS maps. The results are shown in Fig. 5. It can be seen that Ni/Zn/Co/NC is constituted by Co, Ni, C, N, O and Zn elements. Zn and Ni are well loaded and dispersed in the Ni/Zn/Co/NC nanoparticles.

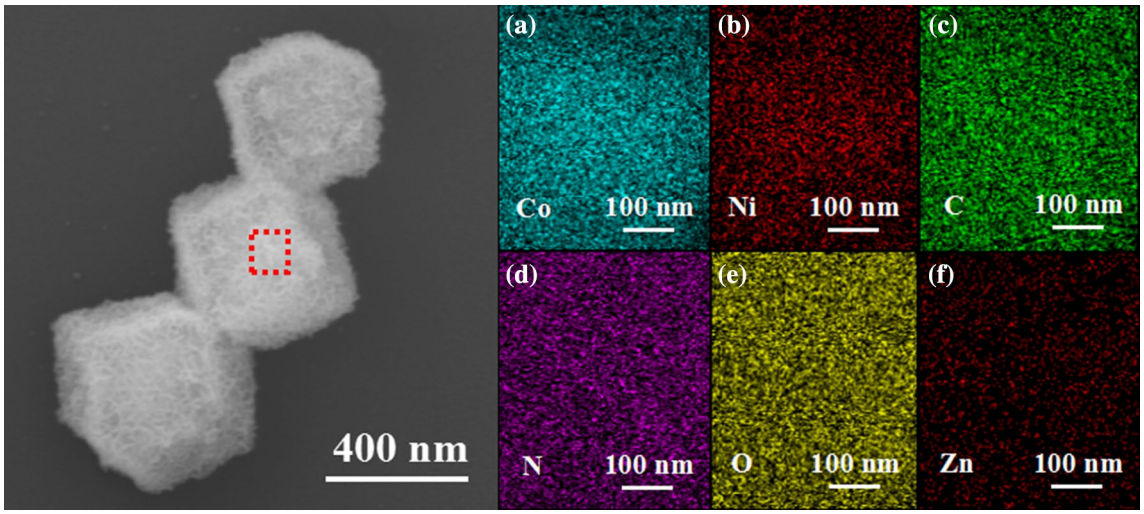

Fig. 5 EDS images of Ni/Zn/Co/NC nanoparticles

The OER activity of the as-synthesized Ni/Zn/Co/NC was evaluated in a standard three-electrode electrochemical cell in alkaline solution (1 M KOH solution). For comparison, Co/NC and Zn/Co/NC were also examined. The results are shown in Fig. 6. Figure 6a is the polarization curves of Co/NC, Zn/Co/NC and Ni/Zn/Co/NC, which are obtained from the linear sweep voltammetry (LSV) curves. The onset potentials of Co/NC and Zn/Co/NC are 1.63 V and 1.58 V, respectively, which are higher than Ni/Zn/Co/NC (1.53 V). Ni/Zn/Co/NC exhibits the lowest onset potential. The superior OER catalytic performance of Ni/Zn/Co/NC may be ascribed to the synergistic effects of Ni, Zn and Co with its porous structure [26–28]. Figure 6b is the Tafel plots of all as-synthesized samples, which are used to investigate the OER kinetics. The Tafel slope of Co/NC, Zn/Co/NC and Ni/Zn/Co/NC is 174, 148 and 112 mV/dec, respectively. It indicates that Ni/Zn/Co/NC shows that fastest kinetics. The results implied that Ni/Zn/Co/NC shows outstanding catalytic performance and possesses the potential to realize the practical applications.

In order to assess the stability of catalyst, Ni/Zn/Co/NC was conducted at a static potential of 1.52 V for 10 h. The result is shown in Fig. 7. As shown in Fig. 7, the required potential of Ni/Zn/Co/NC decreases during the early stage of OER process and then stabilizes. After 10 h of continuous operation, it just shows 4.0% of decay. Ni/Zn/Co/NC exhibits excellent durability for OER in alkaline solution. The excellent durability of Ni/Zn/Co/NC for OER in alkaline solution may be attributed to the structural stability.

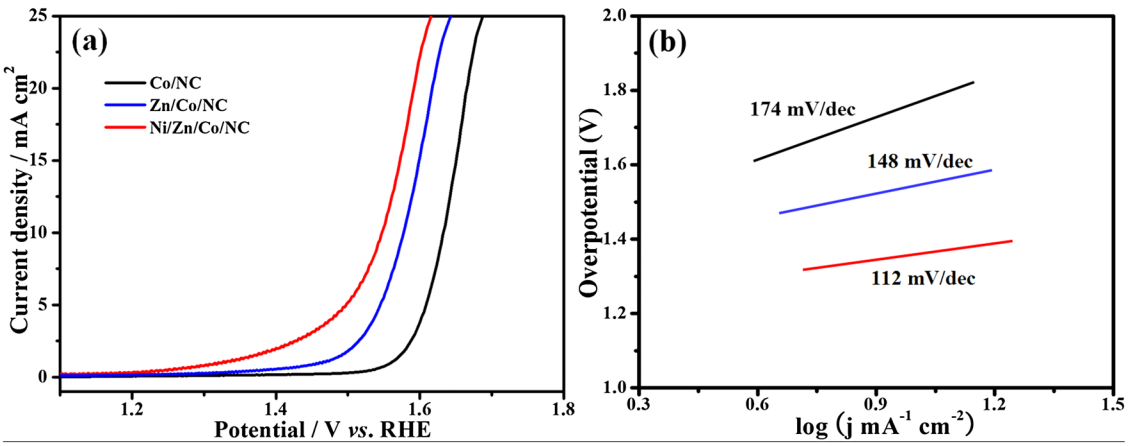

Fig. 6 Palarization curves of and Tafel plots of all catalysts 1 M KOH with 95% IR compensationsin at a scan rate 10 mV/s

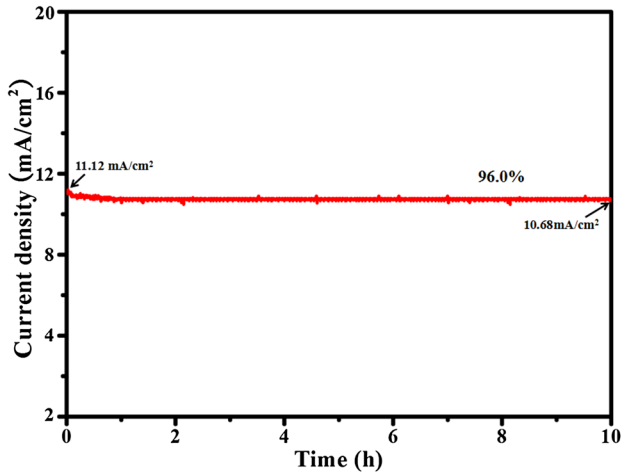

Fig. 7 Chronoamperometry curve for Ni/Zn/Co/NC at a static potential of 1.52 V for 10 h

4 Conclusion

In conclusion, Ni/Zn/Co/NC electrocatalyst was successfully synthesized by using self-templated MOFs. Firstly, ZIF-8/ZIF-67 was synthesized by the facile cocrystallization technique. Then, ZIF-8/ZIF-67 was used as support to prepare Ni doped ZIF-8/ZIF-67 (Ni/ZIF-8/ZIF-67). The thermal annealing treatment was carried out to obtain Ni/Zn/Co/NC electrocatalyst. Benefit from the porous structure and high electroactive sites, the onset potentials of Ni/Zn/Co/NC is 1.53 V, which is lower than the the onset potentials of Co/NC (1.63 V) and Zn/Co/NC (1.58 V). Except that, Ni/Zn/Co/NC has high stability. After 10 h of continuous operation at a static potential of 1.52 V for 10 h, it just shows 4.0% of decay. The excellent OER activity and high stability of Ni/Zn/Co/NC electrocatalyst makes its potential to be used on renewable energy storage and conversion devices.

Acknowledgements The authors grateful acknowledge financial supported by the Open Project Program of Provincial Key Laboratory of Eco-Industrial Green Technology (Wuyi University), the Scientific Technological Innovation Platform of Fujian Province (2014N2013), the Scientific Technological Project of Nanping City [N2015H02, N2012Z06(2)].

References

1. I. Ahmed, J.W. Jun, B.K. Jung, S.H. Jhung, Adsorptive denitrogenation of model fossil fuels with Lewis acid-loaded metal-organic frameworks (MOFs). Chem. Eng. J. **255**, 623–629 (2014)
2. N. Bauer, I. Mouratiadou, G. Luderer, L. Baumstark, R.J. Brecha, O. Edenhofer, Global fossil energy markets and climate change mitigation—an analysis with remind. Clim. Chang. **136**(1), 69–82 (2016)
3. M. Morales, J. Quintero, R. Conejeros., G. Aroca, Life cycle assessment of lignocellulosic bioethanol: environmental impacts and energy balance. Renew. Sustain. Energy Rev. **42**, 1349–1361 (2015)
4. F. Mwasilu, J.J. Justo, E.K. Kim, T.D. Do, J.W. Jung, Electric vehicles and smart grid interaction: a review on vehicle to grid and renewable energy sources integration. Renew. Sustain. Energy Rev. **34**, 501–516 (2014)
5. M.Z. Jacobson, M.A. Delucchi, G. Bazouin, Z.A.F. Bauer, C.C. Heavey, E. Fisher, S.B. Morris, D.J.Y. Piekutowski, T.A. Vencill, T.W. Yeskoo, 100% clean and renewable wind, water, and sunlight (WWS) all-sector energy roadmaps for the 50 United States. Energy Environ. Sci. **8**, 2093–2117 (2015)
6. M. Huber, D. Dimkova, T. Hamacher, Integration of wind and solar power in Europe: assessment of flexibility requirements. Energy **69**, 236–246 (2014)
7. K. Iwashina, A. Iwase, Y.H. Ng, R. Aal, A. Kudo, Z-schematic water splitting into H_2 and O_2 using metal sulfide as a hydrogen-evolving photocatalyst and reduced graphene oxide as a solid-state electron mediator. J. Am. Chem. Soc. **137**, 604–607 (2015)
8. L. Hammarström, Accumulative charge separation for solar fuels production: coupling light-induced single electron transfer to multielectron catalysis. Acc. Chem. Res. **48**, 840–850 (2015)
9. P. Xiao, M.A. Sk, L. Thia, X.M. Ge, R.J. Lim, J.Y. Wang, K.H. Lim, X. Wang, Molybdenum phosphide as an efficient electrocatalyst for the hydrogen evolution reaction. Energy Environ. Sci. **7**, 2624–2629 (2017)
10. J.F. Callejas, C.G. Read, E.J. Popczun, J.M. Mcenaney, R.E. Schaak, Nanostructured Co_2P electrocatalyst for the hydrogen evolution reaction and direct comparison with morphologically equivalent CoP. Chem. Mater. **27**, 3769–3774 (2015)
11. B.S. Lee, H.Y. Park, M.K. Cho, J.W. Jung, H.J. Kim, D. Henkensmeier, S.J. Yoo, J.Y. Kim, S. Park, K.Y. Lee, J.H. Jang, Development of porous Pt/IrO_2 carbon paper electrocatalysts with enhanced mass transport as oxygen electrodes in unitized regenerative fuel cells. Electrochem. Commun. **64**, 14–17 (2016)
12. Y. Hou, Z.P. CheN, D. Wang, B. Zhang, S. Yang, H.F. Wang, P. Hu, H.J. Zhao, H.G. Yang, Highly electrocatalytic activity of RuO_2 nanocrystals for triiodide reduction in dye sensitized solar cells. Small **10**, 484–492 (2014)
13. M. Li, C.P. Feng, W.W. Hu, Z.Y. Zhang, N. Sugiura, Electrochemical degradation of phenol using electrodes of Ti/RuO_2-Pt and Ti/IrO_2-Pt. J. Hazard. Mater. **162**, 455–462 (2009)
14. X.B. Yang, J. Chen, Y.Q. Chen, P.J. Feng, H.X. Lai, J.T. Li, X.T. Luo, Novel Co_3O_4 nanoparticles/nitrogen-doped carbon composites with extraordinary catalytic activity for oxygen evolution reaction (OER). Nano-Micro Lett. **10**, 15 (2018)
15. P. Liu, S. Liu, S.W. Bian, Core-shell-structured Fe_3O_4/Pd@ZIF-8 catalyst with magnetic recyclability and size selectivity for the hydrogenation of alkenes. J. Mater. Sci. **52**, 12121–12130 (2017)
16. Z.C. Miao, F.X. Yang, Y. Luan, X. Shu, D. Ramella, Synthesis of Fe_3O_4@P_4VP@ZIF-8 core-shell microspheres and their application in a Knoevenagel condensation reaction. J. Solid. State. Chem. **256**, 27–32 (2017)
17. X.L. Li, W. Zhang, Y.S. Liu, Palladium nanoparticles immobilized on magnetic porous carbon derived from ZIF-67 as efficient catalysts for the semihydrogenation of phenylacetylene under extremely mild conditions. ChemCatChem **8**, 1111–1118 (2016)
18. X. Liu, J.M. Dong, B. You, Y.J. Sun, Competent overall water-splitting electrocatalysts derived from ZIF-67 grown on carbon cloth. RSC Adv. **6**, 73336–73342 (2016)
19. X.Y. Li, Q.Q. Jiang, S. Dou, L.B. Deng, J. Huo, S.Y. Wang, ZIF-67-derived Co-NC@CoP-NC nanopolyhedra as efficient bifunctional oxygen electrocatalyst. J. Mater. Chem. A **4**, 15836–15840 (2016)
20. Y. Guan, L. Yu, X.W. Lou, Formation of single-holed cobalt/N-doped carbon hollow particles with enhanced electrocatalytic

activity toward oxygen reduction reaction in alkaline media. Adv. Sci. **4**, 1700247 (2017)
21. X.B. Yang, J. Chen, J.P. Hu, S.Y. Zhao, J.Y. Zhao, X.T. Luo, Metal organic framework-derived $Zn_{1-x}Co_x$-ZIF@$Zn_{1-x}Co_xO$ hybrid photocatalyst with enhanced photocatalytic activity through synergistic effect. Catal. Sci. Technol. (2018). https://doi.org/10.1039/CY01979C
22. J.K. Zaręba, M. Nyk, M. Samoć, Co/ZIF-8 heterometallic nanoparticles: control of nanocrystal size and properties by a mixed-metal approach. Cryst. Growth Des. **16**, 6419–6425 (2016)
23. Y.Q. Chen, J.T. Li, G.H. Yue, X.T. Luo, Novel Ag@nitrogen-doped porous carbon composite with high electrochemical performance as anode materials for lithium-ion batteries. Nano-Micro Lett. **9**, 32 (2017)
24. A. Aijaz, J. Masa, C. Rösler, W. Xia, P. Weide, A.J.R. Botz, R.A. Fischer, W. Schuhmann, M. Muhler, Co@Co_3O_4 encapsulated in carbon nanotube-grafted nitrogen-doped carbon phlyhedra as an advanced bifunctional oxygen electrode. Angew. Chem. Int. Ed. **55**, 4087–5091 (2016)
25. A.C. Ferrari, J. Robertson, Interpretation of Raman spectra of disordered and amorphous carbon. Phys. Rev. B **61**, 14095–14107 (2000)
26. X.J. Liu, Z. Chang, L. Luo, T.H. Xu, X.D. Lei, J.F. Liu, X.M. Sun, Hierarchical $Zn_xCo_{3-x}O_4$ nanoarrays with high activity for electrocatalytic oxygen evolution. Chem. Mater. **26**, 1889–1895 (2014)
27. J.T. Zhang, Z.H. Zhao, Z.H. Xia, L.M. Dai, A metal-free bifunctional electrocatalyst for oxygen reduction and oxygen evolution reactions. Nat Nanotechnol. **10**, 444–452 (2015)
28. S. Chen, J.J. Duan, M. Jaroniec, S.Z. Qiao, Nitrogen and oxygen dual-doped carbon hydrogel film as a substrate-free electrode for highly efficient oxygen evolution reaction. Adv. Mater. **26**, 2925–2930 (2014)